UCRL-9587

UNIVERSITY OF CALIFORNIA

Ernest O. Lawrence Radiation Laboratory

BERKELEY, CALIFORNIA

UCRL-9587
Limited Distribution

UNIVERSITY OF CALIFORNIA

Lawrence Radiation Laboratory
Berkeley, California

Contract No. W-7405-eng-48

PION-HYPERON RESONANCES

Margaret H. Alston and Massimiliano Ferro-Luzzi

March 7, 1961

PION-HYPERON RESONANCES

Margaret H. Alston and Massimiliano Ferro-Luzzi

Lawrence Radiation Laboratory
University of California
Berkeley, California

March 7, 1961

PREFACE

This article represents the combined version of two invited papers given by the authors at the Strong Interactions Conference held in Berkeley in December 1960. In particular, one of us (M. F. L.) presented the work performed with the 15-in. hydrogen bubble chamber of the Lawrence Radiation Laboratory at Berkeley by the following physicists and graduate students: P. L. Bastien, J. P. Berge, O. I. Dahl, M. Ferro-Luzzi, W. E. Humphrey, J. Kirz, D. H. Miller, J. J. Murray, A. H. Rosenfeld, R. R. Ross, J. A. Schwartz, F. T. Solmitz, R. D. Tripp, and M. B. Watson. The other author (M. H. A.) discussed the experimental data on Y^* available as of the time of the Conference and in particular the results of an experiment on K^--p interactions at 1.15-Bev/c incident momentum, performed with the same bubble chamber by M. H. Alston, L. W. Alvarez, P. Eberhard, M. L. Good, W. Graziano, H. K. Ticho, and S. G. Wojcicki. Since the two talks were so closely related, they have been combined into the present review article which has been submitted for publication in the Proceedings of the Conference (July issue of Reviews of Modern Physics).

The authors are glad to have this opportunity to thank again all the above-mentioned peope for letting them present the results of these experiments.

PION-HYPERON RESONANCES

Margaret H. Alston and Massimiliano Ferro-Luzzi

Lawrence Radiation Laboratory
University of California
Berkeley, California

March 7, 1961

ABSTRACT

The experimental data available, as of February 1961, on the pion-hyperon resonances are reviewed. The existence of a resonant state in the Λ-π system with a total energy of 1385 Mev and a half width $\Gamma/2$ of about 25 Mev is well-established. This T = 1 resonance should also be observed in the Σ - π system, but the observed Σ/Λ branching ratio is found to be small and consistent with zero. Pion-hyperon resonances have been predicted by both global symmetry and "bound state" $\bar{K}$-N theories. The present data are in agreement with both hypotheses, but allow no discrimination between them.

PION-HYPERON RESONANCES*

Margaret H. Alston and Massimiliano Ferro-Luzzi†

Lawrence Radiation Laboratory
University of California
Berkeley, California

March 7, 1961

I. INTRODUCTION

Recently a resonance in the Λ-π system called Y_1^* has been observed, with a total energy of 1385 Mev.[1-6] This paper will review and discuss the experimental data available as of February 1961. Data from the first two experiments, which were performed at Berkeley using the 15-in. hydrogen bubble chamber, will be discussed in some detail and the data combined wherever possible. Other data will be used to show the effect of the resonance in various interactions.

II. THEORETICAL PREDICTIONS

Resonances in the pion-hyperon system have been predicted and are of two kinds: those arising from global symmetry and those resulting from bound states in the $\bar{K}$ - N system.

Global symmetry predicts two spin-3/2 pion-hyperon resonances,[7] one with isospin T = 1, the other with T = 2. These are the hyperon counterparts of the J = T = 3/2 resonance of the pion-nucleon system. No counterpart can appear in the J = 3/2, T = 0 or in the J = 1/2 states. The relevant kinematical data for the π-N resonance and the π-Y system with T = 1(Y_1^*) are shown in Table I. The T = 1 resonance is predicted with a total energy of about 1375 Mev and a half width $\Gamma/2$ = 23 Mev.[8] The value of the half-width is derived from the observed 45-Mev half-width of the pion-nucleon resonance after correcting for the difference in the c.m. momenta for the two cases $\left[\left(\frac{P_\Lambda}{P_p}\right)^3 = 0.73\right]$ and taking into account the restrictions on the decay rate[9] due to decay into the Σ-π mode $[\frac{2}{3}]$. The Y^* with

T = 1 can decay into either a Λ-π or Σ-π system, the predicted Σ/Λ branching ratio R being about 5 percent for each charge state of the Σ.[9] The T = 2 resonance is expected to have a larger mass value of about 1530 Mev, and a half width of about 60 Mev. The above predictions depend upon the values of the pion-hyperon coupling constants used, and are obtained by assuming that $f^2_{\pi N} = f^2_{\pi\Sigma} = f^2_{\pi\Lambda}$.

In the $\bar{K}$-N "bound-state" model,[10] Λ-π and Σ-π resonances arise from the $\bar{K}$ interactions and are a consequence of the properties of s-wave $\bar{K}$-N scattering. The zero-energy K^-+p data permit a four-fold ambiguity in the solution for the scattering length; only two of the solutions (the "minus" ones) will give Y-π resonances since, to obtain a resonance below the $\bar{K}$-N threshold, the real part of the scattering amplitude must be negative. The a_- solution[11] predicts a T = 1 resonance in both the Λ-π and Σ-π systems at a total energy of 1382±20 Mev with a half width $\Gamma/2$ of 18 Mev and a possible T = 0 resonance at a lower energy. The b_- solution[12] predicts a T = 0 resonance with a total energy near 1420 Mev and possibly a T = 1 resonance at lower energy. In both cases of course, s-wave $\bar{K}$-N bound state has total angular momentum J = 1/2 and breaks up into Λ+π via $S_{1/2}$ wave if the K-Y parity is odd and $P_{1/2}$ if the K-Y parity is even. This model predicts a value of the Σ/Λ branching ratio R of from 15 to 80 percent,[11] the magnitude depending upon the assumptions made and in particular upon the relative Λ-Σ parity.

The experimental data are at present unable to distinguish between the two possible interpretations of the observed resonance, since interference effects (see Section III F) make the determination of the spin and parity inconclusive.

III. THE PRODUCTION OF Y^* IN THE REACTION $K^-+p \to Y^*+\pi$

A. General

The Λ-π resonance has been observed in experiments performed at Berkeley using the 15-inch hydrogen-filled bubble chamber and separated K^-

beams.[13, 14] The first experiment was at 1.15 Bev/c incident K^- momentum.[1] Currently a study[2] of the process for incident K^- momenta from 850 Mev/c down to the Λ-π resonance threshold of 415 Mev/c is being made. In these experiments, Y^* should be observed in the reactions

$$K^-+p \rightarrow \Lambda+\pi^++\pi^- \quad (1)$$
$$\Sigma^0+\pi^++\pi^- \quad (2)$$
$$\Sigma^-+\pi^++\pi^0 \quad (3)$$
$$\Sigma^++\pi^-+\pi^0 \ . \quad (4)$$

A total of about 1000 interactions which appear in the bubble chamber as a two-prong event plus a V have been analyzed. Table II illustrates their apportioning between the various possible reactions. An event was placed in a definite category if the χ^2 probability for other hypotheses was $\leqslant 1$ percent, or was considered ambiguous if both hypotheses (Λ or Σ^0) had a χ^2 probability $\geqslant 1\%$.

B. Dalitz Plots for Reaction (1)

A simple and suggestive way of illustrating the occurrence of the reaction $K^-+p \rightarrow Y_1^{*\pm}+\pi^\pm$ is Dalitz' representation,[15] which consists of displaying the events on a T_{π^+} - T_{π^-} plane (T = kinetic energy in the reaction center of mass). In this plot, unit area is proportional to phase space so that the density of the events is proportional to the matrix element. Thus, if there is no coupling between any two particles in the final state, the points representing the events are expected to lie uniformly over the allowed kinematical region. In contrast to this three-body model, we can consider the two-body reaction in which a Y^*, of fixed mass and zero width, and a pion are produced. In this case, the events must lie on a horizontal or vertical line associated with a unique T_π. Actually, of course, Y^* is a resonance of finite width (Γ) and will not lie on a line but will be spread over a finite band of the Dalitz plot. The relation between pion kinetic energy and Y^* mass is simply

$$\frac{dM_{Y*}}{dT_{\pi}} = - \frac{E}{M_{Y}*}, \qquad (5)$$

where E is the total energy in the c.m. system. dM_{Y*}/dT_{π} goes from -1.1 at P_K = 510 Mev/c to -1.35 at P_K = 1150 Mev/c.

Figures 1 through 5 show these Dalitz plots. All ambiguous (Λ or Σ^0) events were plotted in the 1.15-Bev/c diagram because estimates showed that most of these were Λ's. In the lower momenta plots, no ambiguous events were used. It may be seen that no evidence for pronounced crowding along the predicted lines occurs for the lower momenta while a definite correlation is noticeable at 760, 850, and 1150 Mev/c.

A more qualitative approach is obtained by projecting the points of the Dalitz plots onto either axis. In order to separate Y_1^{*+} from Y_1^{*-} the convention has been adopted of splitting the kinematical area into two equal parts by a 45-deg line and assigning different signs to the events on the two sides. These $T_{\pi}+$ and $T_{\pi}-$ histograms appear in Figs. 6 to 10 where also a phase-space curve has been drawn for comparison. We should comment on the difficulties introduced into these projections by this arbitrary division of the Dalitz plot. It can be seen that at 1150 Mev/c the bands are well separated. At 850 Mev/c they hardly overlap, the 45-deg line does not pass close to many events and the projection is hardly influenced by the division. On the other hand at the two lowest momenta the shape of the resonance is completely mutilated by this procedure. These mutilated projections are presented not because they contribute information on the shape of the resonance, but to illustrate the uncertainties in separating Y^* from background.

C. Mass and Width of Y_1^*

Inspection of Figs. 9 and 10 show no appreciable Y^{*+} - Y^{*-} mass difference. Hence in Fig. 11 the combined $Y_1^{*+} + Y_1^{*-}$ mass spectrum is plotted for 850 Mev/c incident momentum. On this spectrum a background level is indicated and three normalized resonance curves of the form:

$$\frac{dn}{dM} = \frac{\frac{\Gamma}{2}}{(M-1385)^2+\left(\frac{\Gamma}{2}\right)^2} \quad \frac{N}{\pi} \qquad (6)$$

are plotted (some small dependence on the decay momentum has been neglected). The best value of $\Gamma/2$ is about 15 Mev, and the choice of 1385 as a central value appears uncertain by $\leqslant \pm$ 5 Mev. A higher limit on the values of $\Gamma/2$ is about 20 Mev which is obtained when no background is subtracted from the spectrum.

Even this value of $\Gamma/2$ is smaller than that observed for the 1150 Mev/c spectrum (Fig. 12). Here no background has been subtracted and the fitted curve shows $\Gamma/2$ = 32 Mev. The uncertainty on the mass of each Y^* was computed from the fitted track variables and the variance-covariance matrix. For the 850 Mev/c events this uncertainty is typically ±3 to ±5 Mev; for those at 1150 Mev/c, it is typically ±6 to ±10 Mev. There appears to be a definite discrepancy between $\Gamma/2$ as given by the 850 and 1150 Mev/c data. Adair has pointed out that there are reasons why this background may not be flat under the Y_1^* peaks;[4] the resonance curve at 1150 Mev/c could appear too wide just because it is superimposed on a broader maximum in the background. However an even more convincing way of resolving this apparent disagreement results from the analysis of Dalitz and Miller (see Section III F).

D. Y_1^* Excitation Function

To obtain the total cross-section and excitation functions for the reactions (1) and (2), we have estimated the number of ambiguous events that were probably Λ's. For all incident momenta less than 1150 Mev/c, the number of ambiguous events was quite small and they were assigned to definite categories in the ratio of the unambiguous events. However, in the 1150 Mev/c data the number of ambiguous events is large. Estimates showed that, of the 92 ambiguous events, 13 were more probably Σ^0 than Λ. The total cross sections for all reactions are shown in Table III and the cross section for the $\Lambda\pi^+\pi^-$ final state plotted in Fig. 13, which also shows the estimated cross sections for Y_1^{*+} and Y_1^{*-} production.

To obtain these cross sections, we have subtracted the three-particle, final-state background . The cross section $\sigma(Y_1^*)$ at 850 Mev/c can be obtained fairly unambiguously from Fig. 9, which displays dashed lines assumed to be background. We define all excess over background as Y_1^*. For 760 Mev/c (Fig. 8), the above prescription is still fairly satisfactory, but at 620 Mev/c it becomes meaningless. Inspection of Fig. 6 (510 Mev/c) shows that it is artificial to designate as Y_1^{*-} more than two events out of the 16 in the T_{π^+} projection. This gives an upper limit of 0.1 mb for $\sigma(Y_1^{*-})$ at 510 Mev/c. Although no value can be plotted at 620 Mev/c, we believe that it should be quite small because below the Y_1^* threshold (415 Mev/c) the $\Lambda\pi^+\pi^-$ "background" averages about 2 mb and we assume that σ (background) varies fairly smoothly. Also shown on Fig. 13 are the curves for s- and p-wave production of the Y_1^* assuming a two-body final state ($Y_1^*+\pi$). Despite the uselessness of the 620 Mev/c data, the apparently low $\sigma(Y_1^*)$ at 510 Mev/c does suggest that the Y_1^* excitation function is already dominated by p-wave production at 510 Mev/c.

Two reasons for p-wave dominance have been advanced: (1) Dalitz[11] has pointed out that it is natural for pions to be emitted in p-waves by nucleons as for example in the reaction $p+p\rightarrow\pi^++d$. The same mechanism can apply, though perhaps not so strongly, to the reaction $K^-+N\rightarrow\pi+(\bar{K}N)^*\rightarrow\pi+Y^*$ (2) Sawyer[16] has remarked that if Y_1^* is the $P_{3/2}$ global symmetry resonance then the KY^* parity will be the same as the $K\Lambda$ parity (most likely odd). In this case, s-wave Y_1^*

production can only proceed from a $D_{3/2}$ initial state. If $D_{3/2}$ is weakly absorbed p-wave dominance in the final state will be enhanced. Unfortunately both explanations are reasonable, so the suggestion of a p-wave excitation function does not help to resolve the spin and parity of Y^*.

E. Y_1^* Production Angular Distributions and Polarization

If we assume a two-body final state, the production angular distribution can be written in the form $1 + a \cos\theta_{KY*} + b \cos^2\theta_{KY*} + \cdots$, where θ_{KY*} is the Y_1^* production angle. At 1150 Mev/c there is a slight indication of some $\cos^2\theta_{KY*}$ component for Y^{*+}. At the lower momenta b may be considered equal to zero. The experimental values of a are shown in Table IV and indicate negligible deviations from isotropy except at the highest momentum.

The polarization P_{Y^*} of Y_1^* parallel to the normal $\hat{n}$ to the production plane, can be measured by the chain of strong and weak decays: $Y_1^* \Rightarrow \Lambda + \pi$, $\Lambda \rightarrow p + \pi$. Any polarization P_Λ of the Λ will indicate a polarization of the Y^*. The value of $\bar{P}_\Lambda$ can be calculated from the relation

$$\alpha \bar{P}_\Lambda = \frac{3}{N} \sum_{i=1}^{N} (\hat{n} \cdot \hat{p}) \pm \sqrt{\frac{3 - (\alpha \bar{P}_\Lambda)^2}{N}} \tag{7}$$

where $\hat{p}$ is the unit vector along the proton momentum and α is the asymmetry coefficient in Λ decay ($\alpha \sim 1$). Table IV summarizes $\alpha\bar{P}_\Lambda$ obtained from Eq. (7) using only events in which $|\cos\theta_{KY*}| \leqslant 0.85$. This selection was made because of the $\sin\theta_{KY*}$ dependence of P_{Y^*}. The large value of $\alpha\bar{P}_\Lambda$ at 850 Mev/c confirms the evidence from the excitation function that Y_1^*'s (despite their isotropic production angular distribution at 760 and 850 Mev/c) cannot be assumed to be dominantly produced in s-waves.

F. Interference Effects in Y_1^* Production

The oversimplified model in which Y_1^* is produced "isolated" in a two-body final state neglects the interferences (a) between Y_1^* of opposite charge, (b) between Y_1^* and $(\Lambda\pi^+\pi^-)$ produced in nonresonant background states, and (c) final-state interaction between π^+ and π^- and the influence of Bose statistics on this system.

A truly isolated Y_1^* cannot display any fore-aft asymmetry when it strong-decays. A way to measure the departure of the experimental situation from the "isolated" model is offered by the asymmetry coefficient A in the Y_1^* strong-decay distribution:

$$1+A\ \cos\theta_{Y*\Lambda} + B\cos^2\theta_{Y*\Lambda} + \cdots\cdot \qquad (8)$$

where $\theta_{Y*\Lambda}$ is the angle between the Y^* and the Λ in the Y^* c.m. system.

None of our data exhibit any evidence for B=0, but $|A|$ is large (see Table IV) and shows that "isolation" is a poor approximation even at 1150 Mev/c. The sign of A is consistent with the fact that one expects $Y^{*\pm}$ to strong-decay with the Λ going backwards so as to favor resonance with the $\pi^{\mp}$.

Dalitz and Miller are currently making an analysis based on a three-body final state, taking into account the interference effects mentioned, with the exception of the π-π interaction.[17] Preliminary results of this analysis give a satisfactory explanation of most of the experimental data. The difference in the observed width of the resonance at different incident momenta is automatically introduced by the interference mechanism, and the data at all incident momenta are found to be mutually consistent for a half-width of about 25 Mev. The distribution of events on the Dalitz plots allow only two interpretations: s-wave production of an I=1 Y_1^* or p-wave production of an I=0 Y_1^*. The asymmetry coefficients in the Y_1^* decay (Table IV) can also be explained by the model except those at 1150 Mev/c where the effect is larger than that predicted.

G. Adair Analysis for the Spin of Y_1^*

If the model in which the Y_1^* is produced isolated were applicable, an Adair analysis would determine the Y_1^* spin.[18] A polar produced Y_1^* with $J>1/2$ is transversely aligned because there is no component of orbital angular momentum in the beam direction. The decay distribution of this Y_1^* is then uniquely determined by its spin. In particular this distribution will be of the form $1+3\cos^2\theta_{K\Lambda}$ for $J = 3/2$, where $\theta_{K\Lambda}$ is the angle between the beam direction and the decay Λ in the Y* c.m. For $J = 1/2$ the Y_1^* is not aligned and its decay distribution is isotropic.

The experimental data combined for all incident momenta and all Y_1^*'s produced at $|\cos\theta_{KY^*}| \geq 0.90$ are shown in Fig. 14 together with the predicted distributions for $J = 1/2$ and $3/2$. A χ^2 test gives 5:1 odds against $J = 3/2$. This beautiful conclusion unfortunately seems to be completely irrelevant in view of the Dalitz-Miller arguments. Their treatment gives very different Adair distributions from those predicted by the "isolated" model for both $J = 1/2$ and $3/2$. In particular at 850 Mev/c incident momentum an s-wave $P_{3/2}$ Y_1^* and a p-wave $S_{1/2}$ Y_1^* yield two distributions which cannot be distinguished by the available data.

H. The Branching Ratio $R = (Y_1^* \to \Sigma+\pi)/(Y_1^* \to \Lambda+\pi)$

This branching ratio can be investigated by studying the K^-p interactions in which a Σ and two pions are produced. At present the charged Σ events have only been analyzed in the 1.15-Bev/c experiment.[19] The total cross sections for these events are shown in Table V.

Dalitz plots for uncharged Σ production at 760, 850 and 1150 Mev/c and charged Σ production at 1150 Mev/c are shown in Figs. 15 to 19. In order to derive values of R, two corrections were applied to the Σ^0 events. In these cases only about 2/3 of the events are observed, because of neutral decays of the Λ, and some events are not plotted because they have an ambiguous Σ^0 or Λ interpretation. (See Section III A) The plotted events, therefore, were weighted appropriately to obtain the branching ratio R.

An upper limit for R (R_{max} in Table VI) is found by assuming that all events in which the total energy of the Λ-π and Σ-π systems lies between 1355 and 1415 Mev are Y_1^* events. This treatment provides an unrealistic upper limit since there is obviously a large amount of background present. A more realistic value for R is obtained by subtracting a uniform phase-space background. At all incident momenta the results are consistent with R = 0. This small value of the branching ratio for the strong decay of Y_1^* is in poor agreement with the predicted values quoted in the introduction, however, it is more consistent with the global symmetry explanation of the resonance than with the $\bar{K}$-N "bound-state" hypothesis. On the other hand, there seems to be little evidence for a resonance in the Σ-π system at a total energy of about 1540 Mev, as predicted by the global-symmetry argument; but it must be noted that the distribution of events would be very insensitive to the presence of such a wide resonance.

IV. EVIDENCE FOR THE Λ-π RESONANCE IN OTHER INTERACTIONS

A. Deuterium: The Reaction $K^-+d \rightarrow Y^*+p$

In a recent experiment at Berkeley in which K^- mesons were stopped in the deuterium filled 15-inch bubble chamber,[3] the reactions

$$K^-+d \rightarrow \Lambda+\pi^-+p \quad (9)$$

$$\Sigma^0+\pi^-+p \quad (10)$$

$$\Sigma^-+\pi^0+p \quad (11)$$

were studied. The first two reactions can be separated by kinematics unless the recoil proton is too short to be measured. Figure 20 shows the Dalitz plot for

282 events of reaction (9). The proton energy spectrum for these events is plotted in Fig. 21.

The concentration of events in the region of the Dalitz plot where T_p is small and T_π is about 145 Mev can be easily explained. These are the results of K^- absorption on the neutron in the deuteron, in which the proton is a "spectator". An impulse model which assumes the K^- is absorbed from an atomic S orbital and which only includes the Λ-p interaction in the final state is appropriate for this situation because the pion-nucleon system is produced in the weakly interacting T = 1/2 state. The curve A in Fig. 21 shows the expected spectrum; it can be seen that this model fits qualitatively for $T_p < 10$ Mev.

The events with pion energies near 92 Mev are explained by a two-step process in which the K^- interacts with one nucleon to form a Σ and π^- and the Σ then interacts with the other nucleon and is converted to a Λ. Since the conversion occurs mainly in the S-wave state of the Σ-N system, lines of constant T_{π^-} in Fig. 20 will be uniformly populated. The calculated curve B is shown in Fig. 21.

The theory accounts qualitatively for most of the proton and pion spectra but there remains a group of events, with $T_p > 10$ Mev and $T_{\pi^-} < 100$ Mev, which are not explained. These anomalous events can be interpreted as the production of the $\Lambda\pi$ (Y_1^*) resonance. The curve drawn in Fig. 21 shows the effect of the resonance. The mass used is 1382 Mev and the half width 20 Mev. It can be seen that a spectrum obtained by summing curves A, B, and C fits the data remarkably well. From this curve it is estimated that 93 events are associated with the resonant channel, 102 are internal conversions and 87 are directly produced Λ's. Unfortunately the data is insufficient to determine the spin and parity of the Y_1^*. It is estimated that 6 percent of all K^- absorptions proceed through the resonant $\Lambda\pi^-$ channel whereas only 1.2 percent of stopped K's produce hyperons in non-mesic processes.

Reaction (11) was studied to obtain the branching ratio R. The events which are produced by the decay of Y_1^* appear in a region of the proton spectrum ($P_p \sim 240$ Mev/c), which is unpopulated by the direct three-body production process. Twelve events were found with proton momentum > 180 Mev/c giving an upper limit for R of 5 percent.

B. The Reaction $\bar{K}^0 + p \rightarrow Y^* + \pi$

Adair discusses results on this reaction in some detail in one of the previous papers.[4] Again a $\Lambda\pi$ resonance is observed with $M_{Y_1^*} = 1385$ Mev.

C. Helium: $K^- + He^4 \rightarrow Y^* + He^3$

Block et al. have studied 50 events of the type

$$K^- + He^4 \rightarrow \Lambda + \pi^- + He^3 \qquad (12)$$

produced when K^- mesons stopped in Duke University's helium bubble chamber.[5]

An impulse model predicts a phase-space peak in the He^3 momentum spectrum at 126 Mev/c but the experimental peak is at 250 Mev/c. The observed spectrum can be explained by the production of Y_1^* with a mass of 1385 Mev and a width of 20 Mev. The decay angular distribution of the 30 events which have a He^3 momentum greater than 200 Mev/c and which are assumed to be due to Y_1^* production is isotropic. If the K^- is captured from an S orbital and a simple two-body (Y_1^* + He^3) final-state model is used then the decay distribution should be isotropic for a J = 1/2 Y_1^* and of the form $1 + 3\cos^2\theta_{\Lambda Y^*}$ for a Y_1^* of spin 3/2. The result therefore suggests that the spin of the Y_1^* is 1/2. However interference effects in the three-body final state may affect this conclusion. If the $K\Lambda$ parity is odd then a J = 1/2 Y_1^* will be produced in an s state relative to the He^3 and will subsequently decay via $S_{1/2}$ mode.

D. Propane: $K^- + p \rightarrow Y^* + \pi$ or $K^- + n \rightarrow Y^* + \pi$

Preliminary data obtained by the Wilson Powell group[6] using the Berkeley 30-inch propane bubble chamber show evidence, on a total of 60 analysed events, for both Y^{*+}, Y^{*-} and Y^{*0} production in the above reactions.

V. CONCLUSIONS

The existence of the $\Lambda\pi$ resonance, its mass value of 1385±5 Mev and half width of 25±5 Mev appear to be the only noncontroversial results now available. Other properties such as: spin, parity, excitation function and decay branching ratio are inconclusively determined at present. This unsatisfactory situation is mainly due to interference phenomena in the final state which complicate the interpretation of the data. These effects make it necessary to obtain more data; in particular for the K^-p reactions, at incident momenta greater than 1000 Mev/c, where the interference effects should be of less importance.

This lack of a conclusive interpretation of the experimental data leaves the theoretical explanation of the resonance an open question.

ACKNOWLEDGMENTS

The authors are indebted to the many experimenters who furnished their data and allowed them to be included here. In particular we would like to thank R. H. Dalitz, D. H. Miller, and A. H. Rosenfeld for their comments and advice.

FOOTNOTES

†National Academy of Sciences Fellow.

*Work done under the auspices of the U.S. Atomic Energy Commission.

1. Margaret Alston, Luis W. Alvarez, Philippe Eberhard, Myron L. Good, William Graziano, Harold K. Ticho, and Stanley G. Wojcicki, Phys. Rev. Letters 5, 520 (1960).

2. J. P. Berge, M. Ferro-Luzzi, D. H. Miller, J. J. Murray, A. H. Rosenfeld, F. T. Solmitz, and R. D. Tripp, To be published in Phys. Rev. Letters.

3. O. Dahl, N. Horwitz, D. H. Miller, J. J. Murray, and P. G. White, Phys. Rev. Letters 6, 142 (1961).

4. R, K. Adair, talk presented at the Strong Interactions Conference, Berkeley, California Dec. 1960.

5. M. M. Block, private communication.

6. R. P. Ely, S. Y. Fung, G. Gidal, Y. L. Pan, W. M. Powell, and H. White, private communication.

7. M. Gell-Mann, Phys. Rev. 106, 1296 (1957).

8. D. Amati, B. Vitale, and A. Stanghellini, Phys. Rev. Letters 5, 524 (1960).

9. If we assume global symmetry, the branching ratios are
$Y_1^{*\pm} \Longrightarrow \Lambda+\pi^{\pm} : \Sigma^{\pm}+\pi^0 : \Sigma^0+\pi^{\pm} = 4 : 1 : 1$ and
$Y_1^{*0} \Longrightarrow \Lambda+\pi^0 : \Sigma^0+\pi^0 : \Sigma^++\pi^- : \Sigma^-+\pi^+ = 4 : 0 : 1 : 1.$
Of course the relative Σ ratios are independent of global-symmetry arguments and follow from charge independence only. The Σ/Λ branching ratios then have to be corrected by the appropriate phase-space factor[$(P_\Sigma/P_\Lambda)^3 = 0.23$, see Table I].

10. R. H. Dalitz and S. F. Tuan, Phys. Rev Letters 2, 425 (1959); Annals of Physics 8, 100 (1959); Annals Phys. 10, 307 (1960).

11. R. H. Dalitz, submitted to Phys. Rev. Letters.

12. R. L. Schutt and R. H. Capps, private communication.

13. P. Eberhard, M. L. Good, H. K. Ticho, Rev. Sci. Instr. 31, 1054 (1960).

14. P. Schlein, P. Bastien, O. Dahl, J. J. Murray, M. Watson, R. G. Ammar, paper presented at the International Conference on Instrumentation for High-Energy Physics, Berkeley 1960.

15. M. Gell-Mann and A. H. Rosenfeld, Annual Review of Nuclear Science, Vol. 7 (Annual Reviews Inc., Palo Alto, California, 1957), p. 407 (Appendix C).

16. R. F. Sawyer, private communication by M. L. Good.

17. R. H. Dalitz and D. Miller, to be published.

18. R. K. Adair, Phys. Rev. 100, 1540 (1955).

19. M. Alston, L. W. Alvarez, P. Eberhard, M. L. Good, W. Graziano, H. K. Ticho, and S. G. Wojcicki, to be published in Phys. Rev. Letters.

Table I. Kinematical data for the pion-nucleon J = 3/2, T = 3/2 resonance and the pion-hyperon J = 3/2, T = 1 resonance.

Strong decay	Q (Mev)	P_π, c. m. (Mev/c)		Γ/2 (Mev)
$N^*_{3/2} \rightarrow N + \pi$	159	230	$\left(\frac{P_\Lambda}{P_N}\right)^3 = 0.73$	45[a]
$Y^*_1 \rightarrow \Lambda + \pi$	130	207	$\left(\frac{P_\Sigma}{P_\Lambda}\right)^3 = 0.23$	23[b]
$Y^*_1 \rightarrow \Sigma + \pi$	50	127		

[a] Experimental value

[b] Predicted value

Table II. Distribution of events and cross sections (in parentheses) among different reactions for different values of the incident K^- momentum, P_K

Reaction	Distribution at: 510 Mev/c	620 Mev/c	760 Mev/c	850 Mev/c	1150 Mev/c
$K^- + p \rightarrow \Lambda + \pi^+ + \pi^-$	30 (1.5±.3)	54 (2.1±.3)	262 (3.6±.3)	153 (3.5±.3)	49 (4.1±.4)
$(\Lambda \text{ or } \Sigma^0) + \pi^+ + \pi^-$	2	2	41	37	92
$\Sigma^0 + \pi^+ + \pi^-$	9	10	51	35	27
$(\Lambda \text{ or } \Sigma^0) + \pi^+ + \pi^- + \pi^0$	0 (0)	0 (0)	20 (0.20±.05)	7 (0.11±.04)	39 (1.1±.2)
$\overline{K}^0 + p + \pi^-$	0 (0)	0 (0)	2 (0.03±.02)	3 (0.03±.02)	48 (2.0±.3)
Total events	41	66	376	235	255

Table III. Number of events and cross sections (in parentheses) for Y^* production at different values of the incident K^- momentum.

		Distribution of events			
Reaction	510 Mev/c	620 Mev/c	760 Mev/c	850 Mev/c	1150 Mev/c
$\Lambda\pi^+\pi^-$ { Y^{*-}	< 2 (0.1)		121 (1.2±0.14)	56 (0.9±0.25)	75 (1.8±0.3)
Y^{*+}	< 2 (0.1)	56 (1.8±0.3)	122 (1.2±0.14)	62 (1.0±0.25)	53 (1.3±0.2)
Three-body	> 28(1.0)		56 (0.6±0.1)	67 (1.0±0.15)	0

Table IV. Asymmetry coefficients and Λ polarization in Y^* production and decay for three incident momentum values.

Measured parameters (%)	Coefficients at:					
	760 Mev/c		850 Mev/c		1150 Mev/c	
	Y^{*+}	Y^{*-}	Y^{*+}	Y^{*-}	Y^{*+}	Y^{*-}
Production						
a	10 ± 20	-4 ± 20	2 ± 26	-10 ± 24	-40 ± 26	-30 ± 20
Decay						
A	-24 ± 20	-16 ± 20	-92 ± 26	-34 ± 24	-70 ± 26	-2 ± 20
Λ polarization						
$\alpha \bar{P}_\Lambda$	-16 ± 20	$+10 \pm 20$	$+12 \pm 28$	-56 ± 20	$+2 \pm 22$	-30 ± 20

Table V. Number of events and cross sections (in parenthesis) for Σ production at different values of the incident K^- momentum.

Reaction	Distribution of events				
	510 Mev/c	620 Mev/c	760 Mev/c	850 Mev/c	1150 Mev/c
$\Sigma^0\pi^+\pi^-$	9 (0.2 ± 0.1)	10 (0.3 ± 0.1)	55 (0.6 ± 0.1)	39 (0.6 ± 0.1)	40 (1.0 ± 0.2)
$\Sigma^-\pi^+\pi^0$	a ——	a ——	a ——	a ——	55 (0.8 ± 0.1)
$\Sigma^+\pi^-\pi^0$	a ——	a ——	a ——	a ——	57 (0.8 ± 0.1)

[a]Not yet analysed.

Table VI. Values of the branching ratio R for various incident K^- momenta.

K^- momentum (Mev/c)	R (%)	R_{max}[c] (%)
760[a]	1 ± 3	20
850[a]	-5 ± 5	10
1150[b]	1 ± 3	8.5

a. $R = [Y^{*\pm} \rightarrow (\Sigma^0 + \pi^\pm)] / [Y^{*\pm} \rightarrow (\Lambda + \pi^\pm)]$ at P_{K^-} = 760 and 850 Mev/c.

b. $R = \frac{1}{2} [Y^{*\pm} \rightarrow (\Sigma^0 + \pi^\pm) + (\Sigma^\pm + \pi^0)] / [Y^{*\pm} \rightarrow (\Lambda \pm \pi^\pm)]$ at P_{K^-} = 1150 Mev/c.

c. R_{max} assumes that all the events with $1355 < M_{Y^*} < 1415$ are Y^*'s.

FIGURE LEGENDS

Fig. 1. Dalitz plot for the reaction $K^-+p\rightarrow\Lambda+\pi^++\pi^-$ at P_{K^-} = 510±20 Mev/c (31 events).

Fig. 2. Dalitz plot for the reaction $K^-+p\rightarrow\Lambda+\pi^++\pi^-$ at P_{K^-} = 620±15 Mev/c (54 events).

Fig. 3. Dalitz plot for the reaction $K^-+p\rightarrow\Lambda+\pi^++\pi^-$ at P_{K^-} = 760±7.5 Mev/c (262 events).

Fig. 4. Dalitz plot for the reaction $K^-+p\rightarrow\Lambda+\pi^++\pi^-$ at P_{K^-} = 850±10 Mev/c (153 events).

Fig. 5. Dalitz plot for the reaction $K^-+p\rightarrow\Lambda+\pi^++\pi^-$ at P_{K^-} =1150±25 Mev/c (141 events).

Fig. 6. Pion kinetic energy spectra in c.m. for the reaction $K^-+p\rightarrow\Lambda+\pi^++\pi^-$ at P_{K^-} = 510±20 Mev/c. Only negative (positive) pions belonging to events in the A (B) region of the corresponding Dalitz plot appear in the histograms. The phase-space curve indicates the amount of distortion introduced by this separation. The dotted lines correspond to M_Y*=1385±15 Mev.

Fig. 7. Pion kinetic energy spectra in c.m. for the reaction $K^-+p\rightarrow\Lambda+\pi^++\pi^-$ at P_{K^-} = 620±15 Mev/c. Only negative (positive) pions belonging to events in the A (B) region of the corresponding Dalitz plot appear in the histograms. The phase-space curve indicates the amount of distortion introduced by this separation. The dotted lines correspond to M_Y* = 1385±15 Mev.

Fig. 8. Pion kinetic energy spectra in c.m. for the reaction $K^-+p\rightarrow\Lambda+\pi^++\pi^-$ at P_{K^-} = 760±7.5 Mev/c. Only negative (positive) pions belonging to events in the A (B) region of the corresponding Dalitz plot appear in the histograms. The phase-space curve indicates the amount of distortion introduced by this separation. The dotted lines correspond to M_Y* = 1385±15 Mev.

Fig. 9. Pion kinetic energy spectra in c.m. for the reaction $K^- + p \rightarrow \Lambda + \pi^+ + \pi^-$ at P_{K^-} = 850±10 Mev/c. Only negative (positive) pions belonging to events in the A (B) region of the corresponding Dalitz plot appear in the histograms. The phase-space curve indicates the amount of distortion introduced by this separation. The dotted lines correspond to M_{Y^*} = 1385±15 Mev.

Fig. 10. Pion kinetic energy spectra in c.m. for the reaction $K^- + p \rightarrow \Lambda + \pi^+ + \pi^-$ at P_{K^-} = 1150±25 Mev/c. Here no division between Y^* charges has been made; curves drawn are undistorted phase space.

Fig. 11. Y^* mass spectrum from 226 $\Lambda\pi^+\pi^-$ events at P_{K^-} = 850 Mev/c.

Fig. 12. Y^* mass spectrum from 141 $\Lambda\pi^+\pi^-$ events at P_{K^-} = 1150 Mev/c.

Fig. 13. Excitation data for the total $\Lambda\pi^+\pi^-$ production and its apportioning into Y^{*+} and Y^{*-}. The dashed curves are P_{Y^*}(c.m.) and $P^3_{Y^*}$ (c.m.) as a function of P_{K^-}(lab). Points at 300 and 400 Mev/c represent very preliminary values.

Fig. 14. Adair analysis for Y^* at P_{K^-} = 760, 850 and 1150 Mev/c, and $|\cos\theta_{KY^*}| \geq 0.90$.

Fig. 15. Dalitz plot for the reaction $K^- + p \rightarrow \Sigma^0 + \pi^+ + \pi^-$ at P_{K^-} = 760±7.5 Mev/c (55 events).

Fig. 16. Dalitz plot for the reaction $K^- + p \rightarrow \Sigma^0 + \pi^+ + \pi^-$ at P_{K^-} = 850±10 Mev/c (39 events).

Fig. 17. Dalitz plot for the reaction $K^- + p \rightarrow \Sigma^0 + \pi^+ + \pi^-$ at P_{K^-} = 1150±25 Mev/c (27 events).

Fig. 18. Dalitz plot for the reaction $K^- + p \rightarrow \Sigma^+ + \pi^- + \pi^0$ at P_{K^-} = 1150± 25 Mev/c (57 events).

Fig. 19. Dalitz plot for the reaction $K^- + p \rightarrow \Sigma^- + \pi^+ + \pi^0$ at P_{K^-} = 1150±25 Mev/c (55 events).

Fig. 20. Dalitz plot for the reaction $K^-+d \rightarrow \Lambda+\pi^-+p$ at $P_{K^-} = 0$ (282 events).

Fig. 21. Proton kinetic energy spectrum for the reaction $K^-+d \rightarrow \Lambda+\pi^-+p$ at $P_{K^-} = 0$.

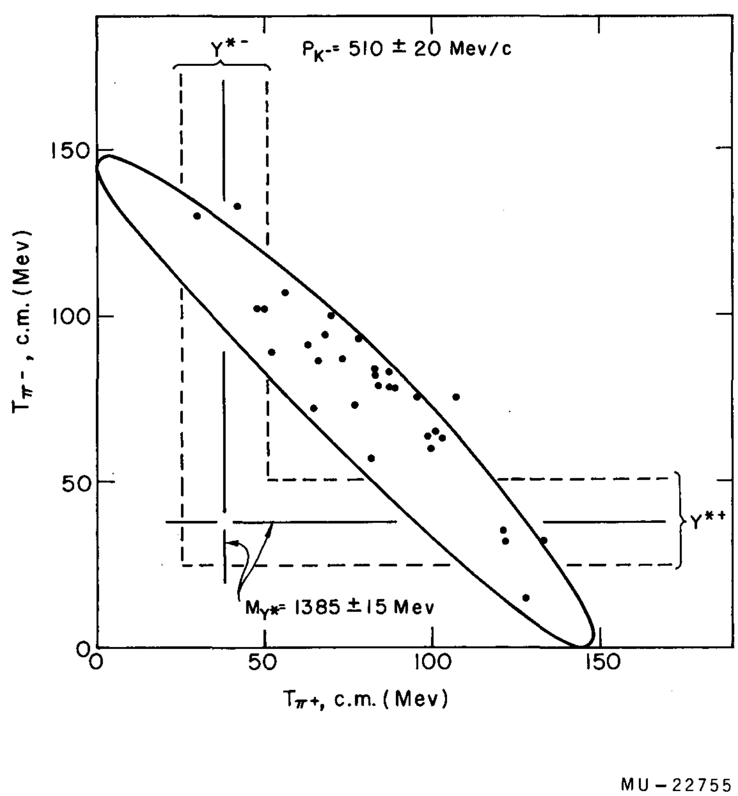
Y*-
P_{K^-}= 510 ± 20 Mev/c
150
100
50
0
0
50
100
150
T_{π^-}, c.m. (Mev)
T_{π^+}, c.m. (Mev)
Y*+
M_{Y^*}= 1385 ± 15 Mev
MU-22755

Fig. 1

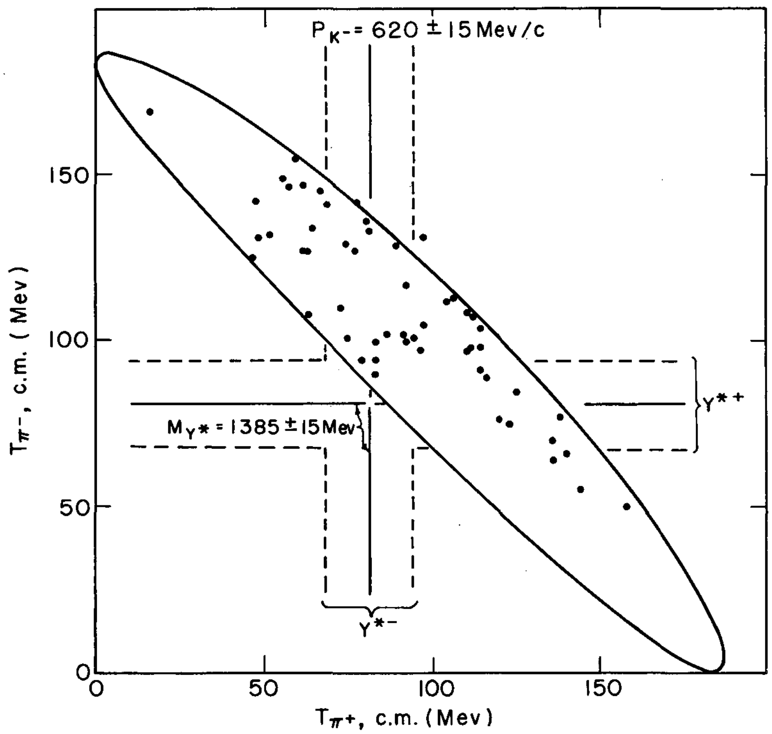

MU-22754

Fig. 2

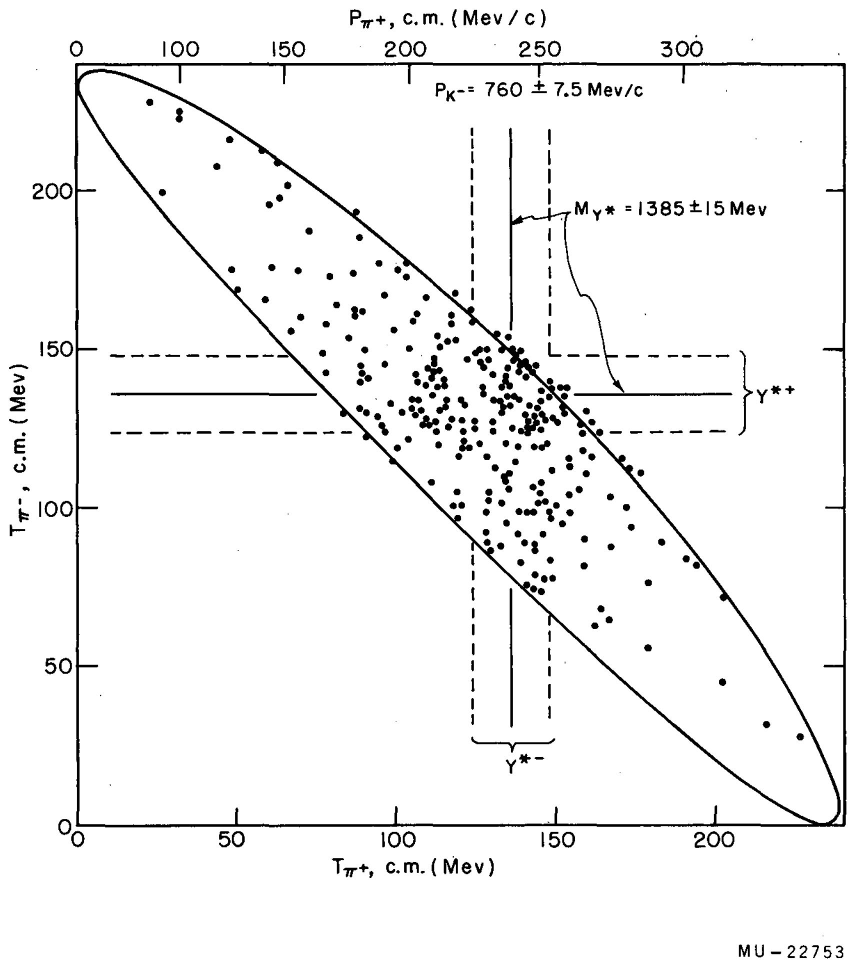
P_π+, c.m. (Mev / c)
0
100
150
200
250
300
P_K- = 760 ± 7.5 Mev/c
M_Y* = 1385 ± 15 Mev
Y*+
Y*-
T_π-, c.m. (Mev)
0
50
100
150
200
T_π+, c.m. (Mev)
MU-22753

Fig. 3

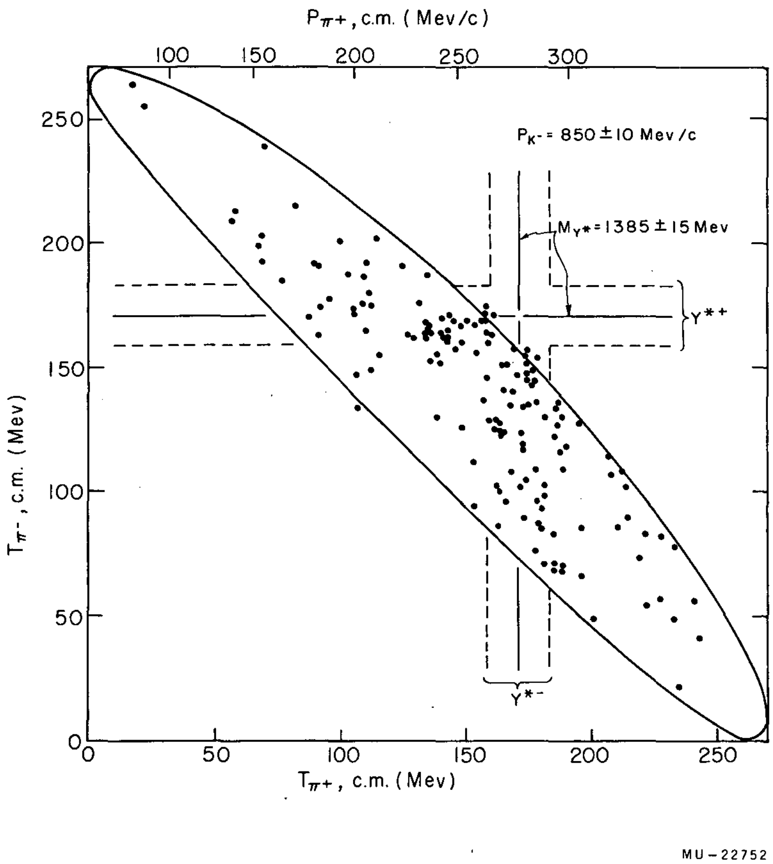
P_{π^+}, c.m. (Mev/c)
100 150 200 250 300
$P_{K^-} = 850 \pm 10$ Mev/c
$M_{Y^*} = 1385 \pm 15$ Mev
Y^{*+}
Y^{*-}
T_{π^-}, c.m. (Mev)
0 50 100 150 200 250
T_{π^+}, c.m. (Mev)
0 50 100 150 200 250
MU-22752

Fig. 4

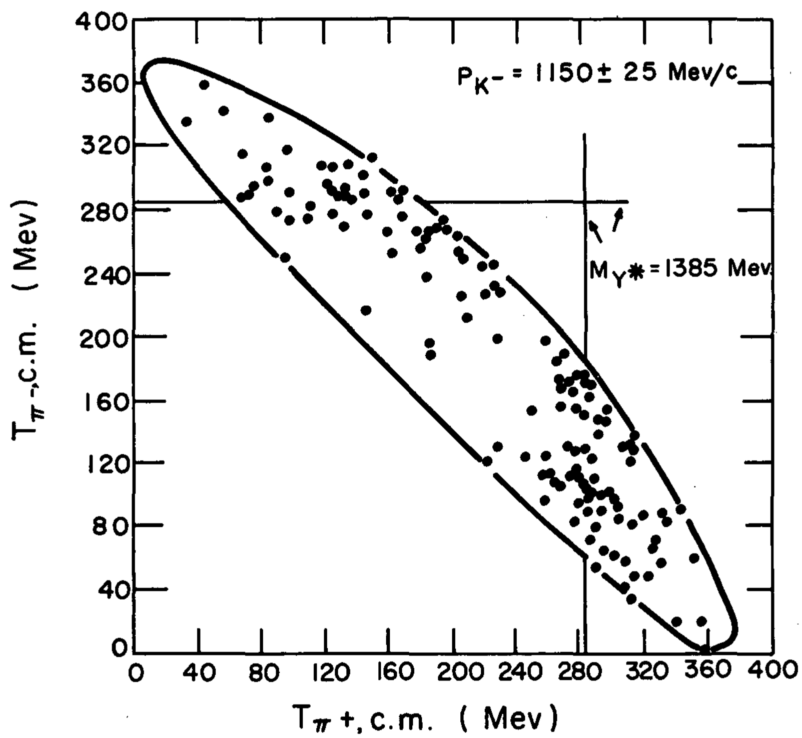

MU-22736

Fig. 5

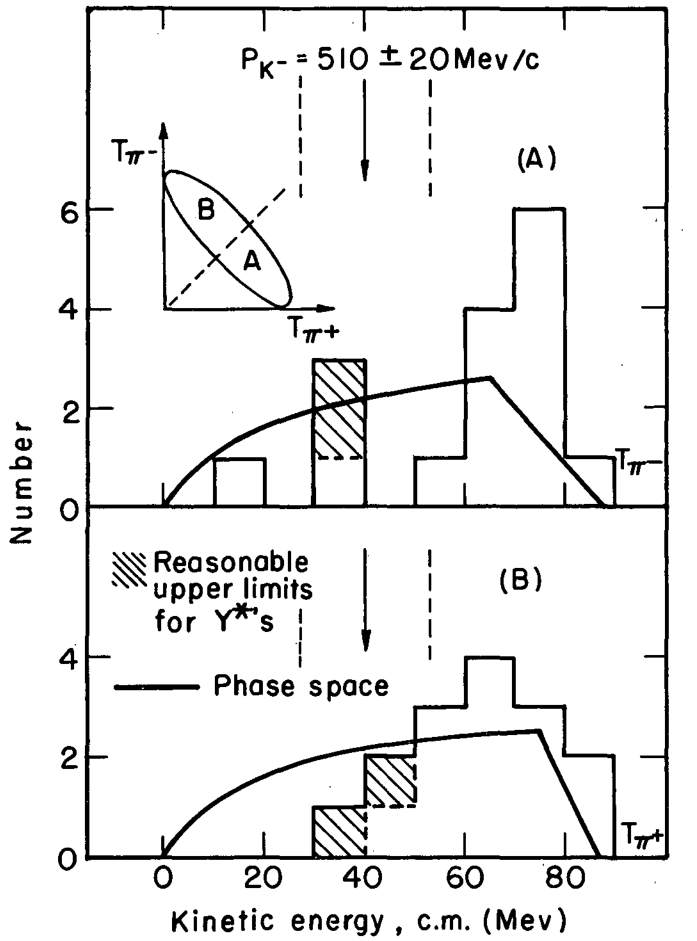

MU-22751

Fig. 6

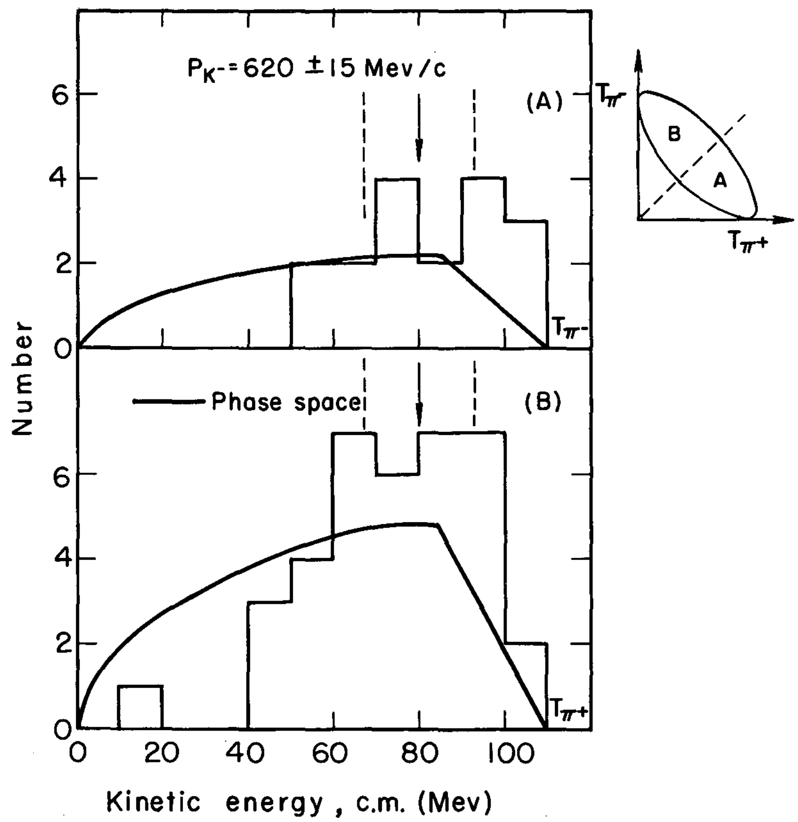

MU-22750

Fig. 7

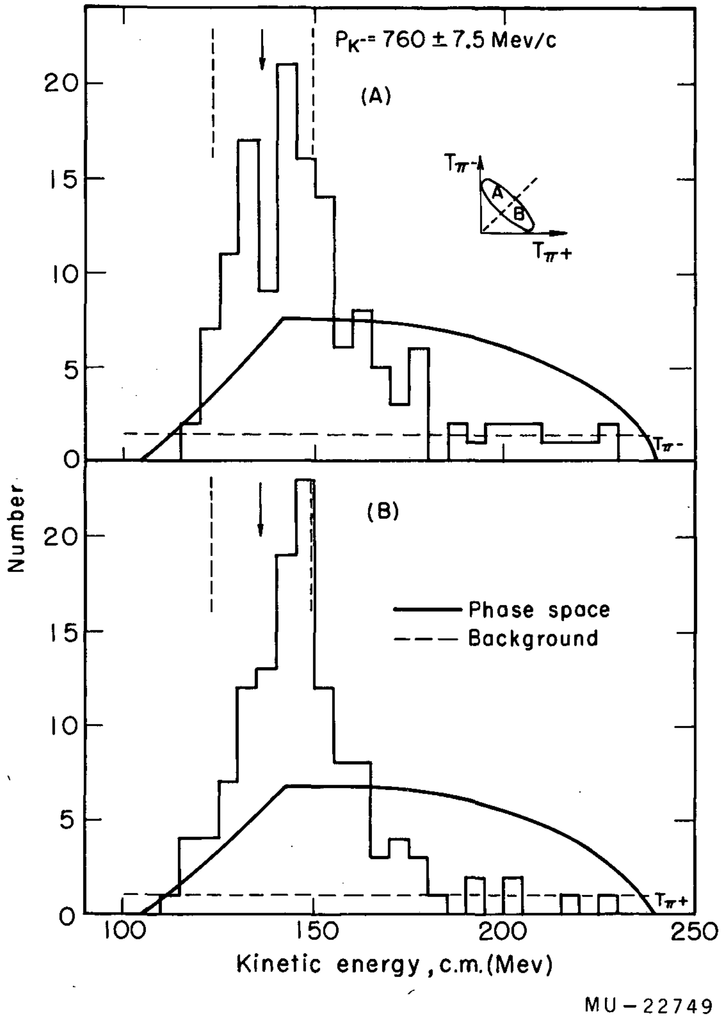
P_{K^-} = 760 ± 7.5 Mev/c
(A)
(B)
T_{π^-}
T_{π^+}
A
B
Phase space
Background
Number
Kinetic energy, c.m.(Mev)
0
5
10
15
20
100
150
200
250
MU-22749

Fig. 8

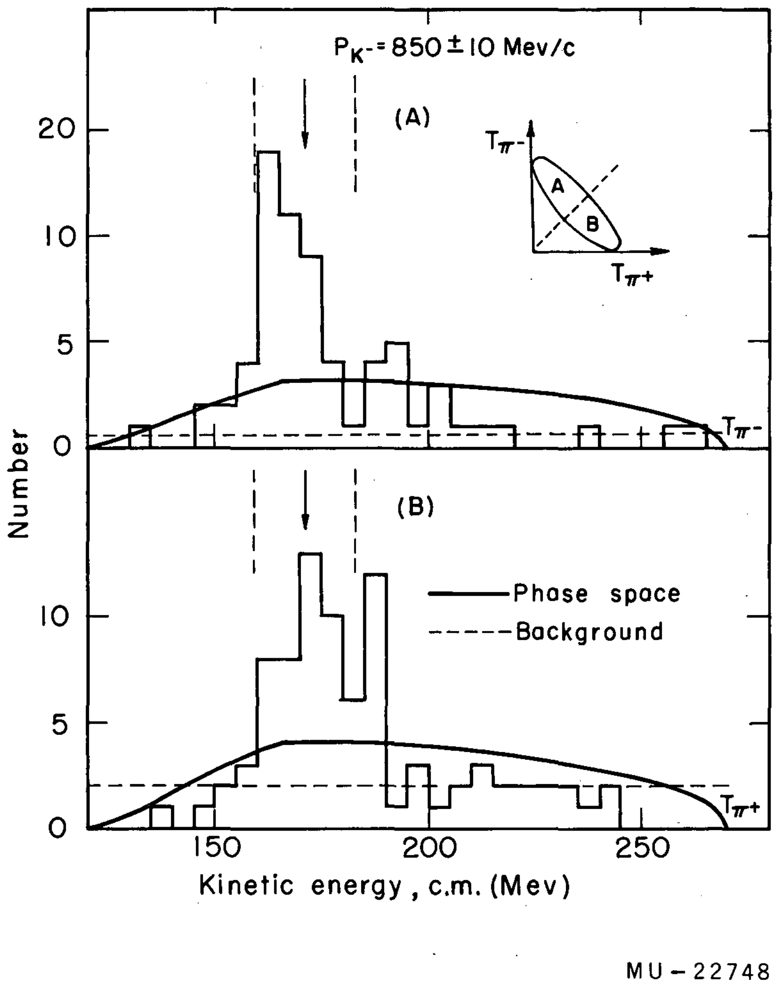
P_{K^-} = 850 ± 10 Mev/c
(A)
T_{π^-}
A
B
T_{π^+}
20
10
5
0
Number
(B)
Phase space
Background
10
5
0
150
200
250
Kinetic energy, c.m. (Mev)
T_{π^-}
T_{π^+}
MU-22748

Fig. 9

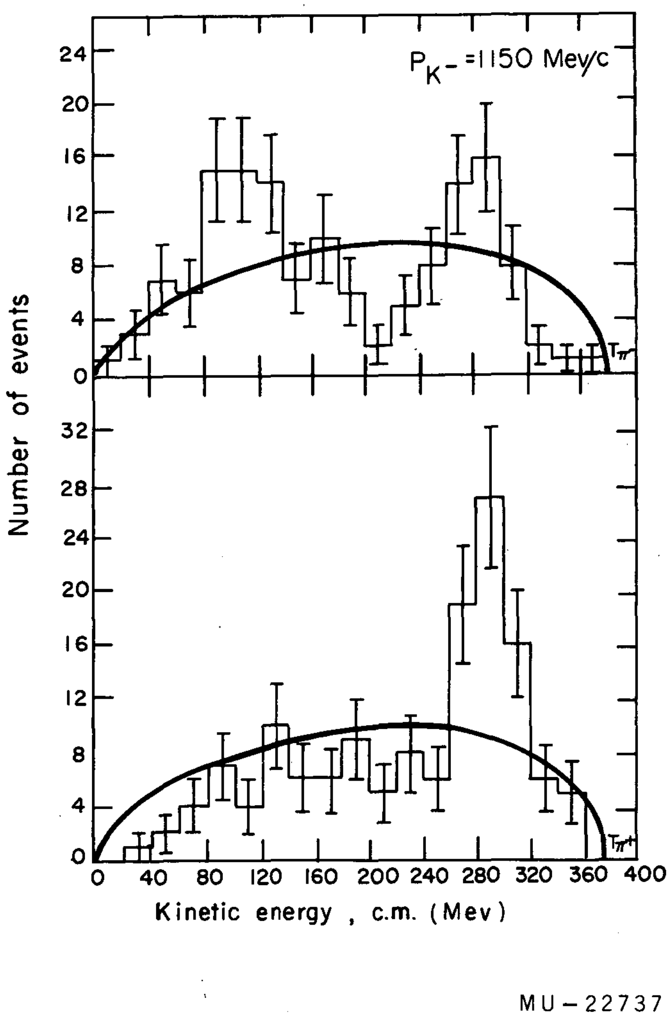
P_{K^-} =1150 Mev/c
Number of events
Kinetic energy , c.m. (Mev)
0
40
80
120
160
200
240
280
320
360
400
4
8
12
16
20
24
28
32
T_{π^-}
T_{π^+}
MU-22737

Fig. 10

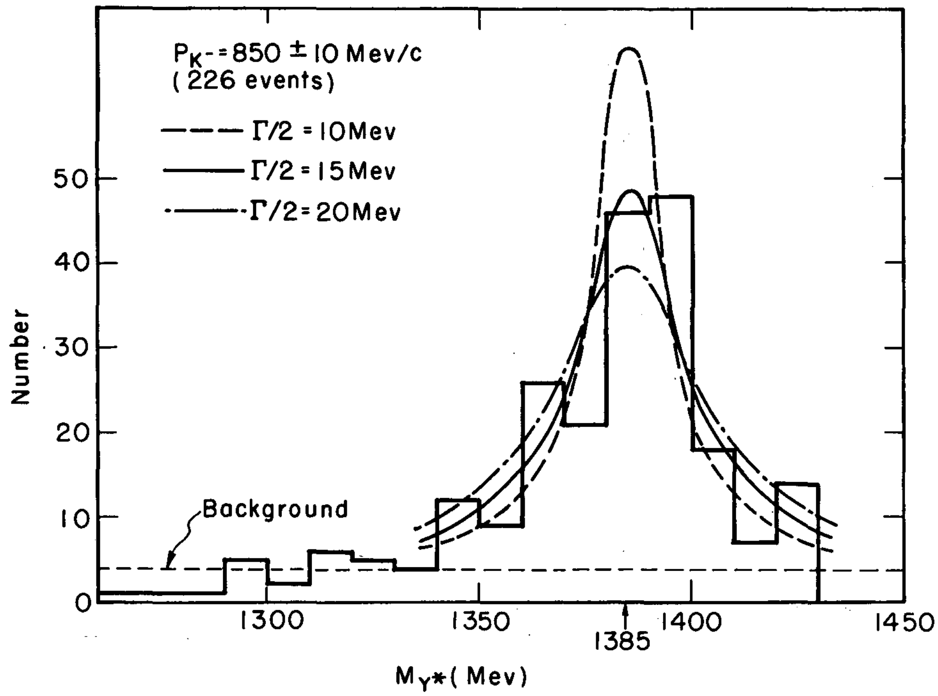

MU-22747

Fig. 11

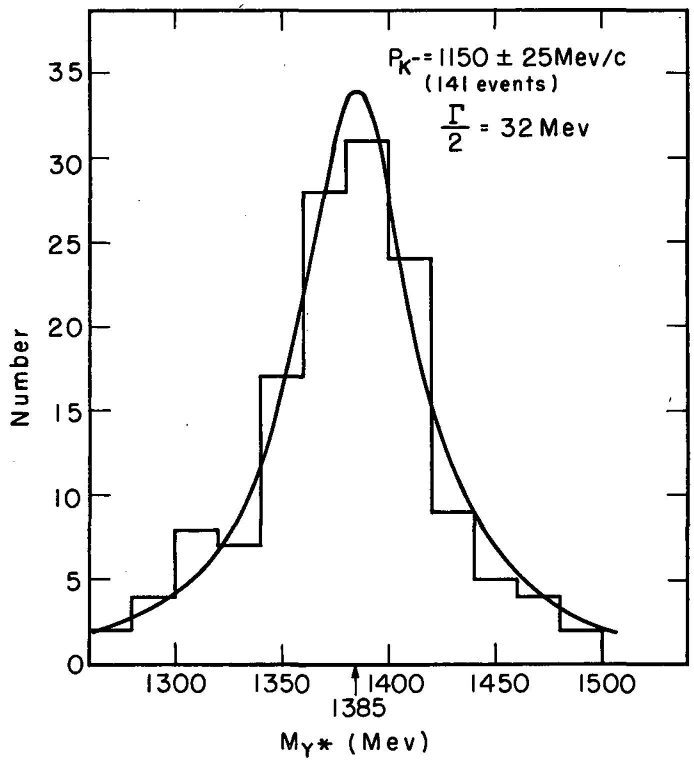

MU-22760

Fig. 12

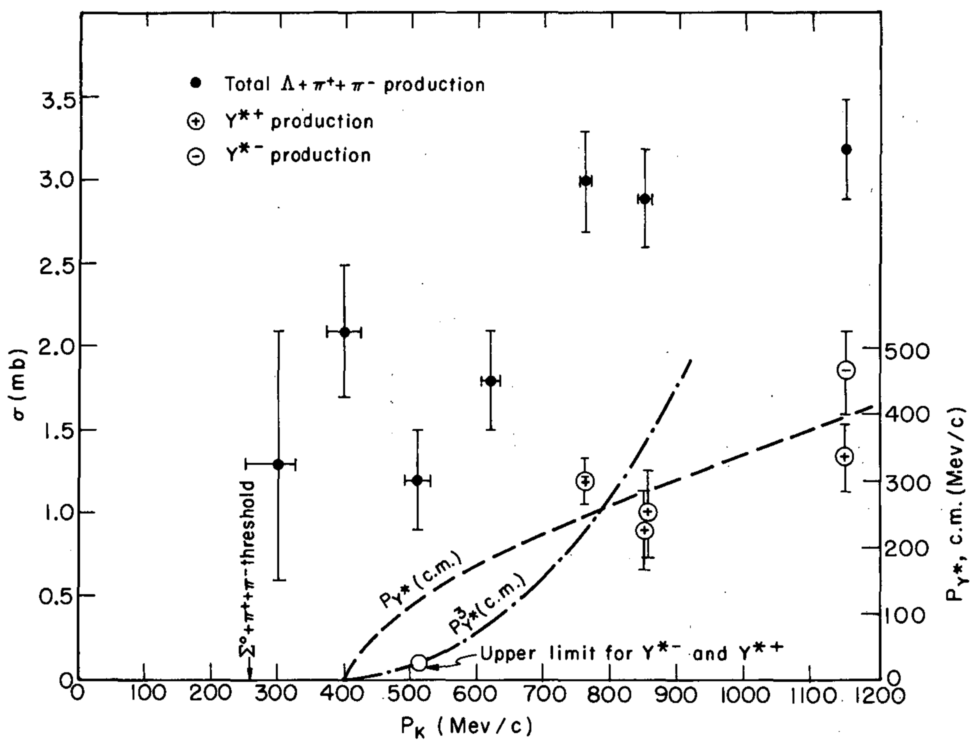
Total $\Lambda+\pi^++\pi^-$ production
Y^{*+} production
Y^{*-} production
σ (mb)
P_{Y^*}, c.m. (Mev/c)
P_K (Mev/c)
$\Sigma^0+\pi^++\pi^-$ threshold
P_{Y^*} (c.m.)
$P^3_{Y^*}$ (c.m.)
Upper limit for Y^{*-} and Y^{*+}
MU-22745

Fig. 13

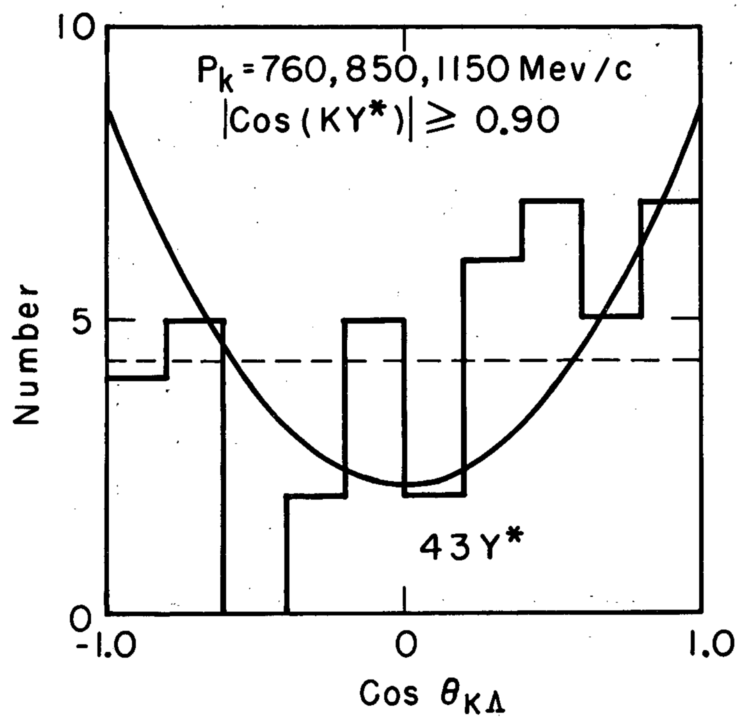
10
5
0
Number
-1.0
0
1.0
Cos $\theta_{K\Lambda}$
P_k = 760, 850, 1150 Mev/c
|Cos (KY*)| ≥ 0.90
43 Y*
MU-22738

Fig. 14

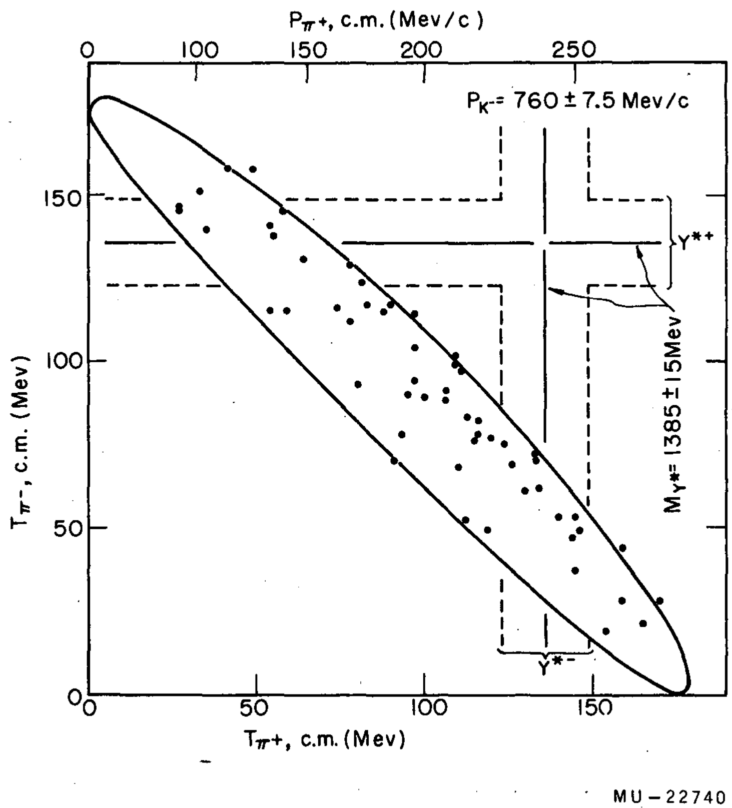
P_{π^+}, c.m. (Mev/c)
0
100
150
200
250
P_{K^-} = 760 ± 7.5 Mev/c
Y^{*+}
M_{Y^*} = 1385 ± 15Mev
T_{π^-}, c.m. (Mev)
150
100
50
0
Y^{*-}
0
50
100
150
T_{π^+}, c.m. (Mev)
MU-22740

Fig. 15

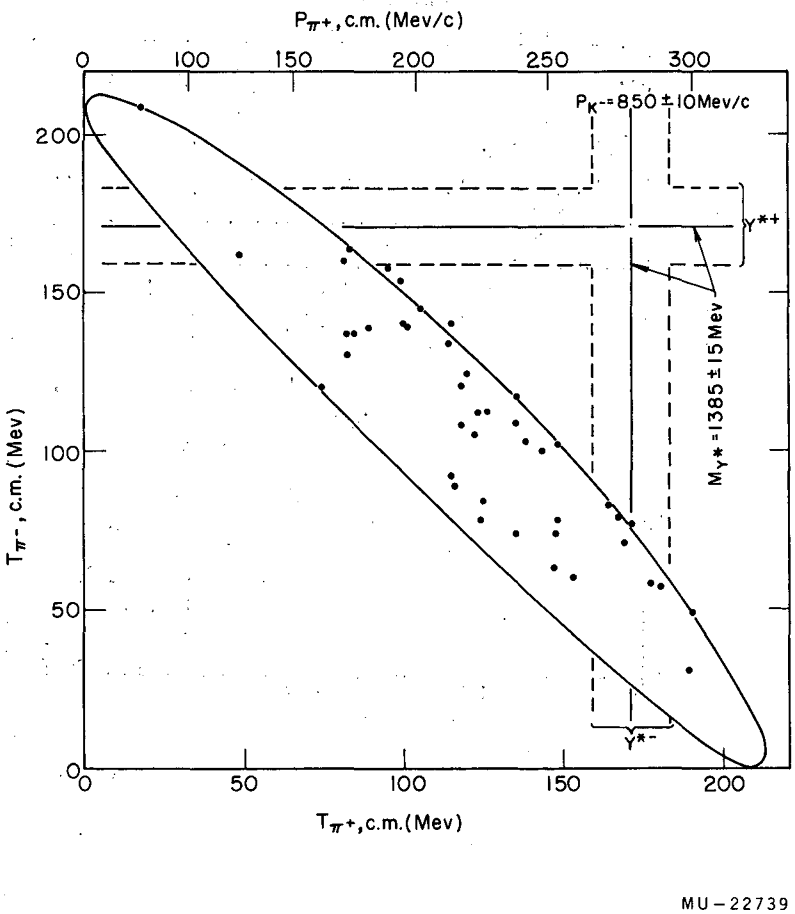
P_{π^+}, c.m. (Mev/c)
0
100
150
200
250
300
P_{K^-}=850 ± 10 Mev/c
Y^{*+}
M_{Y^*} =1385 ± 15 Mev
Y^{*-}
T_{π^-}, c.m. (Mev)
200
150
100
50
0
T_{π^+}, c.m. (Mev)
0
50
100
150
200
MU-22739

Fig. 16

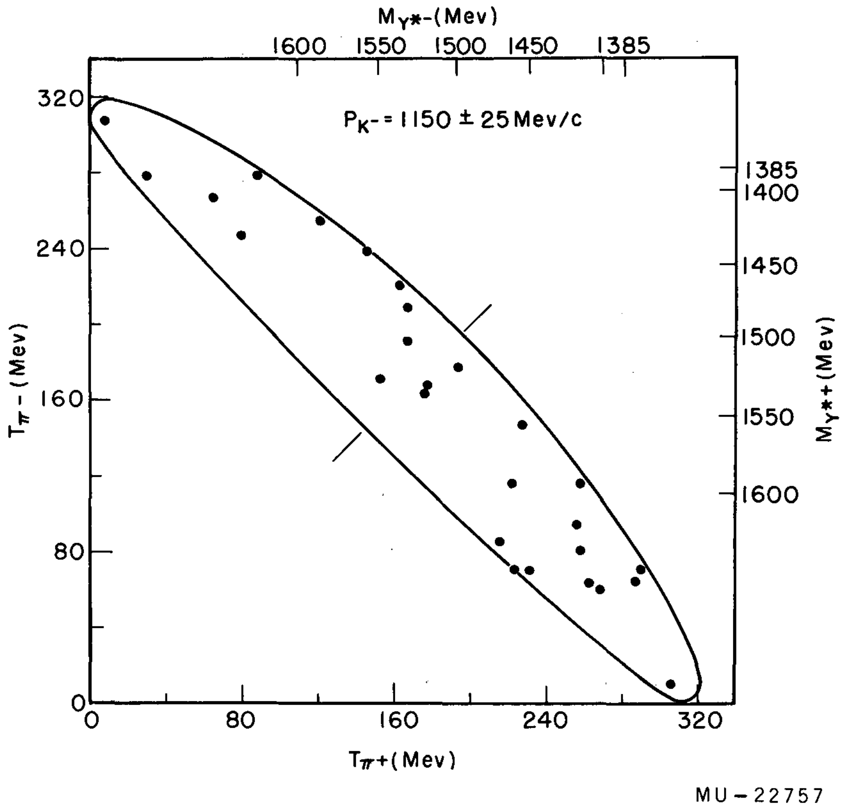
M_{Y*}-(Mev)
1600 1550 1500 1450 1385
P_{K^-} = 1150 ± 25 Mev/c
320
240
160
80
0
0 80 160 240 320
T_{π^-}(Mev)
T_{π^+}(Mev)
1385
1400
1450
1500
1550
1600
M_{Y*}+(Mev)
MU-22757

Fig. 17

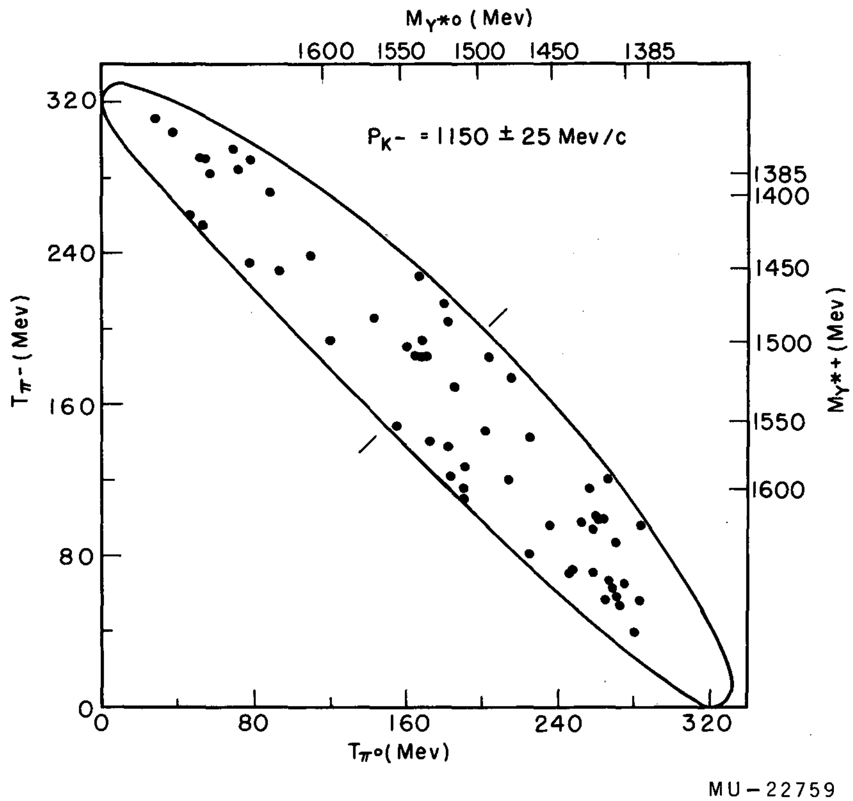
M$_{Y^{*0}}$ (Mev)
1600 1550 1500 1450 1385
P_{K^-} = 1150 ± 25 Mev/c
320
240
160
80
0
T_{π^-} (Mev)
1385
1400
1450
1500
1550
1600
$M_{Y^{*+}}$ (Mev)
0 80 160 240 320
T_{π^0} (Mev)
MU-22759

Fig. 18

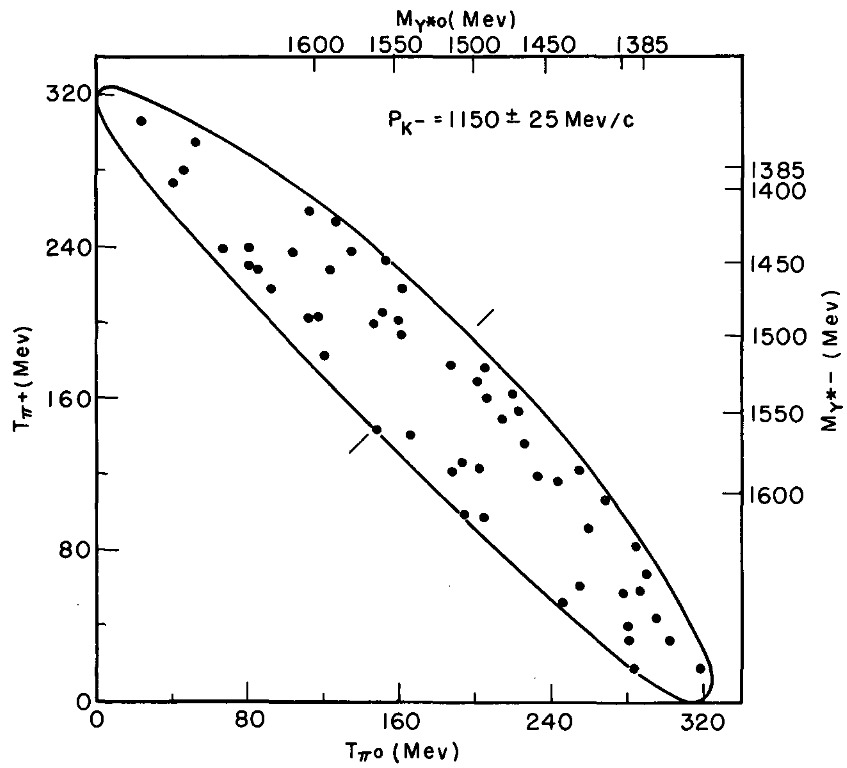

MU-22758

Fig. 19

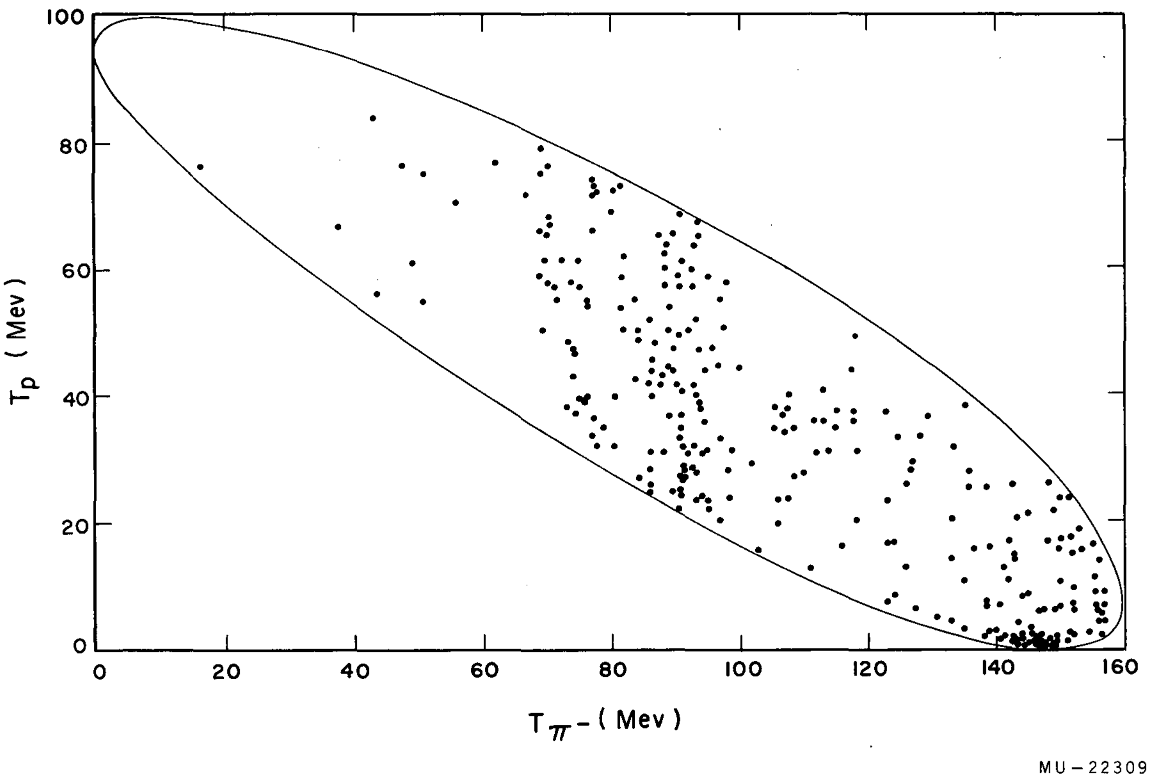
100
80
60
40
20
0
T_p (Mev)
0
20
40
60
80
100
120
140
160
T_{π^-} (Mev)
MU-22309

Fig. 20

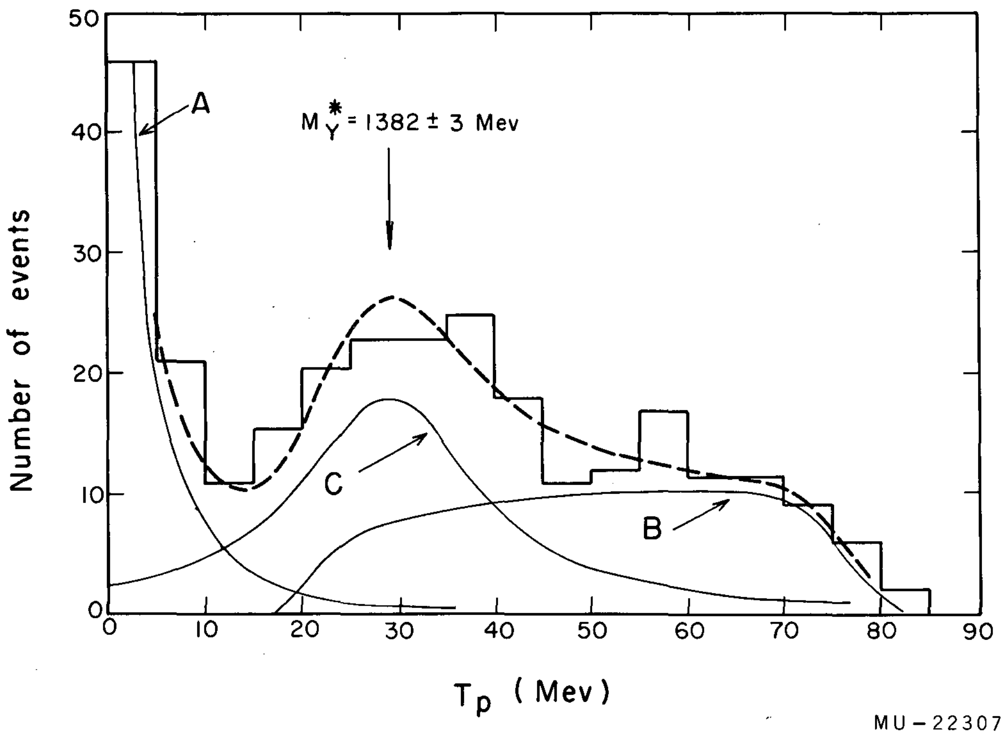
50
40
30
20
10
0
0
10
20
30
40
50
60
70
80
90
Number of events
Tp (Mev)
A
B
C
M_Y^* = 1382 ± 3 Mev
MU-22307

Fig. 21